Chapter 7

Results and Discussion

This chapter will review the main results that were generated from the developed MATLAB Solver; `OS_SQ_Stratified_Solver.m`. The results were found from varying the main inputs, while fixing the Schmid number at 700 (as discussed earlier). Likewise, from the convergence study discussed in the previous section, the number of Chebyshev grid points was fixed to a value of 100. The remaining input parameters that were varied are $(\alpha, \beta, Re, F_h, \theta)$ for a chosen base profile; either pCf or pPf. With these parameters, the most unstable eigenmode was extracted, $\omega_{i,max}$. Likewise, the eigenfunctions of the most unstable eigenmode could be outputted should the user request it.

Given time, a broad range of tilt angles could have been studied to fully investigate the inalignment influences. However, due to time restricts, the main angles that were investigated were 5, 30, 60, 80 degrees, where 5 and 80 degrees were to represent a small and heavy tilt angle. This would give us a strong indication of how the behaviour of the flow evolves from the aligned stratification case to the spanwise case.

The results were categorised into varying certain input parameters while holding the remaining parameters constant. Firstly, the outputted eigenspectra was examined to provide an insight on the features of the complex frequency. Next, the wavenumbers were swept to find the region where instabilities are found. As stated by Deloncle, Chomaz and Billant (2006), two-dimensional instabilities are not expected to dominate, hence reinforcing an interest in three-dimensional turbulence thus non-zero values of (α, β). Next the influence of the tilt angle on the critical Reynolds number, Re_{crit} shall be analysed. Furthering our interest in Re, investigation on the influence of Re on the growth rate is carried out. After that, the F_h effects are examined and finally investigation of the eigenfunctions allow the visualisation of the perturbations providing an idea on the stability mechanisms. Finally, brief comments on the influence of Sc shall be included.

7.1 Eigenspectra

Below plots of the eigenspectra for the pCf and pPf are presented in Figures 7.1 and 7.2 respectively. The input parameters where $(Re, F_h) = (10000, 1)$ for both base flows and the wavenumbers were $(\alpha, \beta) = (0.8, 5)$ for the pCf and $(\alpha, \beta) = (1.5, 6)$ for the pPf. These wavenumbers were chosen as these are the primary regions of instability that appears as the tilt angle increases. This will be made clearer in the neutral stability plots to be presented in Section 7.2. The tilt angle was varied and the subplots in the Figures show the results for $\theta = 5$, 30, 60 and 80 degrees. Both Figures have red points which represents the most unstable eigenmode.

Observing Figure 7.1, one can notice how the eigenspectra has a symmetrical feature with respect to the

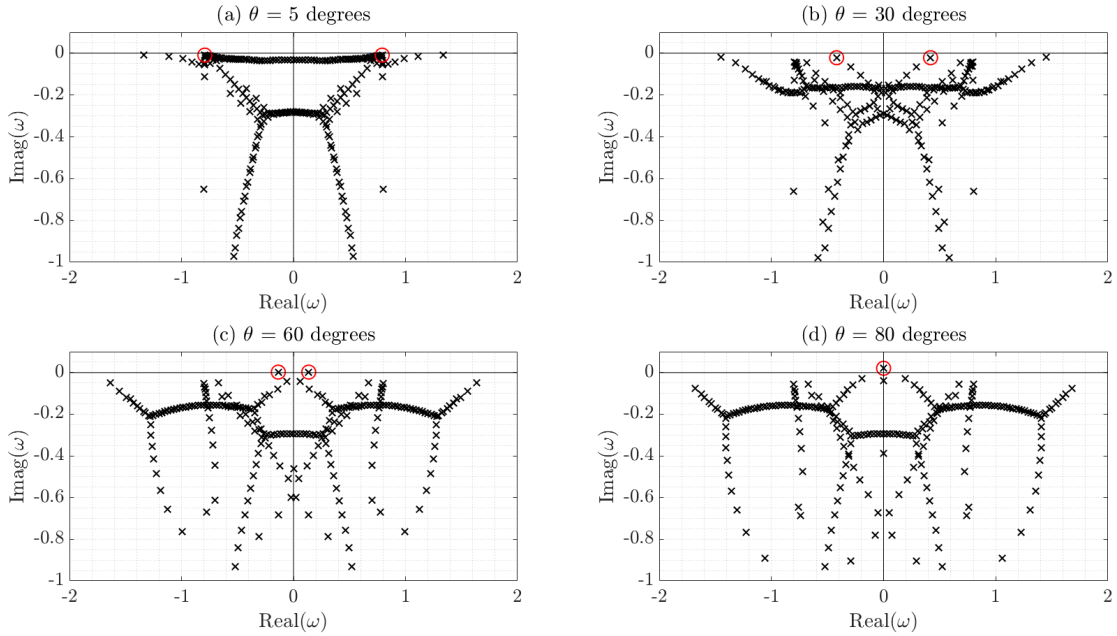

Figure 7.1: Eigenspectra of the pCf base fluid with inputs $(\alpha, \beta, Re, F_h) = (0.8, 5, 10000, 1)$ with subplots of varying tilt angle θ.

real axis, where for a certain growth rate, there is a conjugate pair. One can observe how the eigenmodes break down into various branches as the inalignment is strengthened. This illustrates how the shear and stratification tilt produces more complex flow structures. However, the most significant eigenmode is with most unstable growth rate (highlighted in red). The value of ω_i becomes more positive as the tilt angle is raised. This suggests that the inalignment has a destabilising consequence to the base flow. Notice how as the tilt angle increases, the oscillatory frequency of the most unstable mode (ω_r) decreases in magnitude, as the conjugate pairs move closer together. Between the inalignment angle; 60 degrees and 80 degrees, the most unstable eigenmodes coalesce to produce a single unstable eigenmode with zero oscillatory frequency. Facchini (2018) found the same result, that at 90 degrees, for the critical (Re, F_h), the single unstable mode was non-oscillatory. It is key to note that the instability does not arise at the moment of coalescence, as through observing Figure 7.1(c), the two conjugate eigenmodes are in the upper half plane.

Now looking at Figure 7.2, the symmetry of the eigenvalues does not appear. The eigenspectra is dominated in the lower right plane, with an array of eigenmodes with positive ω_r and stable ω_i. Like the pCf, the most unstable eigenmode becomes more unstable as the tilt angle increases, so the stratification shear inalignment continues to destablise the pPf base flow as well. Moreover, as the tilt angle increases, the eigenspectra splits into multiple branches which also shows the increase in complexity of the perturbations as the tilt angle increases. This displays signs of consistency of the influence of stratification inalignment to the stabililty of shear flows. However, unlike the pCf, there only exists a single unstable mode at all tilt angles.

Note that the symmetrical and assymmetrical features of the eigenspectra, for the pCf and pPf respectively, is also found in the unstratified case with the Orr-Sommerfeld and Squire system, shown in Figures 6.4 and 6.5.

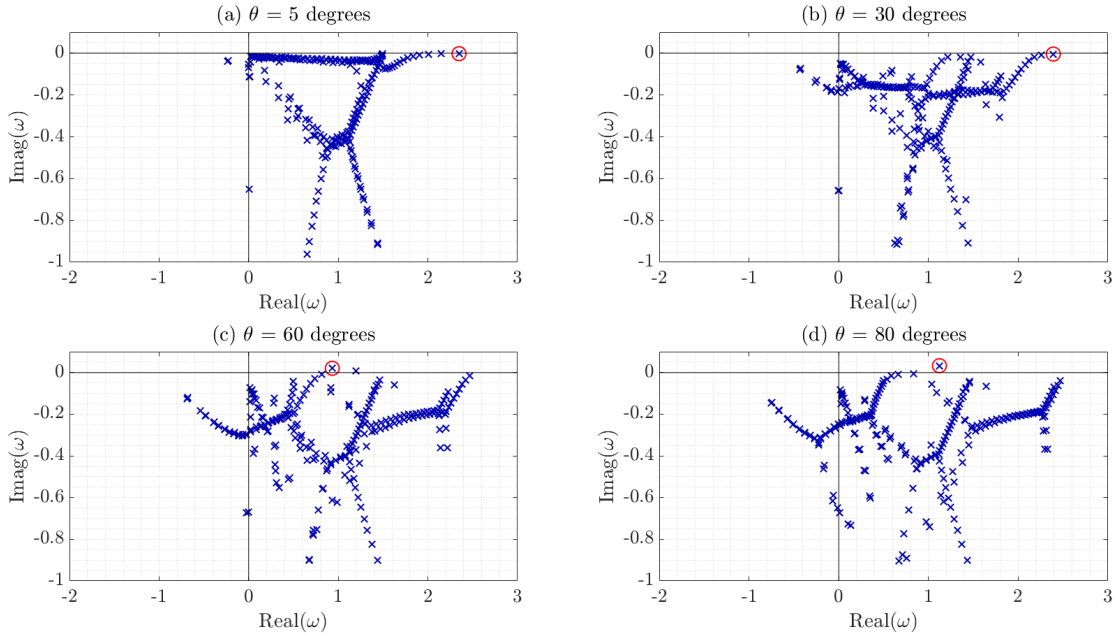

Figure 7.2: Eigenspectra of the pPf base fluid with inputs $(\alpha, \beta, Re, F_h) = (1.5, 6, 10000, 1)$ with subplots of varying tilt angle θ.

7.2 Sweeping Wavenumbers, (α, β)

As a first result, it would be useful to find the region of instability in the wavenumber state space. Therefore, this requires neutral stability plots which are shown in Figures 7.3 to 7.6.

To this end, the stratified solver was run sequentially for a range of wavenumbers while fixing parameters $(Re, F_h, \theta) = (10000, [1, 0.5], [5, 30, 60, 80])$. Figures 7.3 and 7.4 are for the pCf and Figures 7.5 and 7.6 are for the pPf. In these Figures, subplot (a) represents a tilt angle of 60 degrees and (b) with a tilt angle of 80 degrees. Note that results for an inalignment of 5 and 30 degrees has not been shown, as the flow was found to always be stable in these cases. This result is consistent with what was found in the eigenspectra plots of Section 7.1. Notice each of the plots exhibit a red cross. This point represents the most unstable eigenmodes. It is interesting to note that this point is the same for each base flow, which suggests the most unstable point is independent of F_h and θ.

Observing Figure 7.3, the instability bubble is found around the range of wavenumbers $(\alpha, \beta) = ([0.7, 0.8], [4, 5])$. As the tilt angle increases, the instability bubble appears around this region and exhibits slow growth, in the wavenumber plane, which continues until the stratification is aligned spanwise. The area of this instability region is relatively small compared with the pPf cases suggesting that stratified pCf instability is uncommon.

Next, looking at the influence of F_h, by comparing Figures 7.3 and 7.4, increasing the stratification appears to destabilise the flow for a certain tilt angle as the instability region is of a higher area. The increase in the range of instability is small in α, however for β the flow destablises for almost seven times the range when F_h was decreased from 1 to 0.5. To give us a deeper understanding of this finding, further analysis on the influence of F_h to the stability of tilted stratifed shear will be included in Section 7.4.

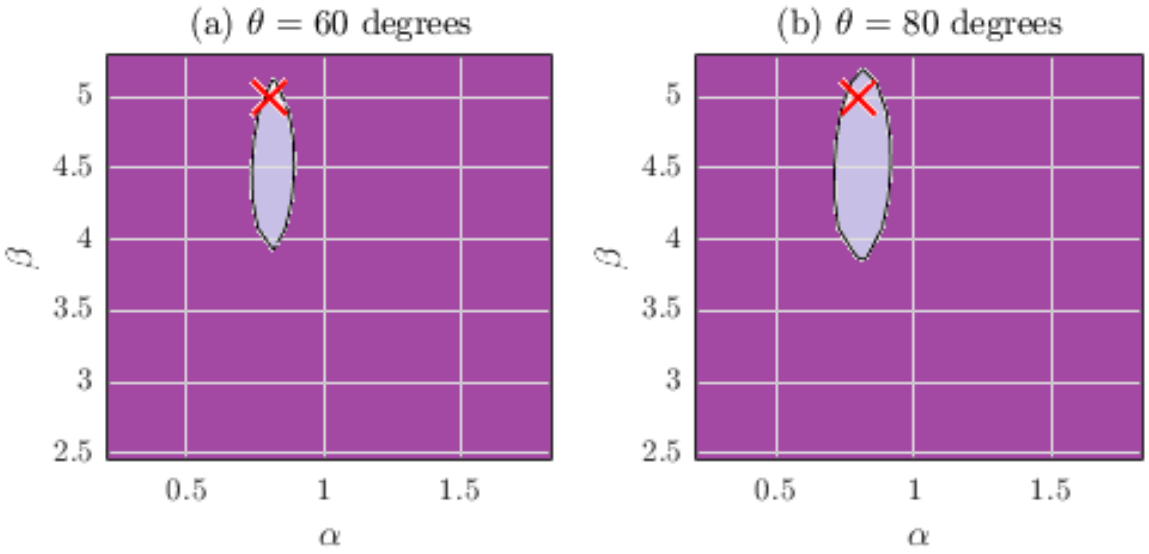

Figure 7.3: Neutral stability plots in the wavenumber state space for the pCf. The instability region is shown in light purple, with the dark purple region being the stable area. The red cross marks the most unstable point. The input parameters were $(Re, F_h) = (10000, 1)$ and (a) $\theta = 60$ degrees, (b) $\theta = 80$ degrees.

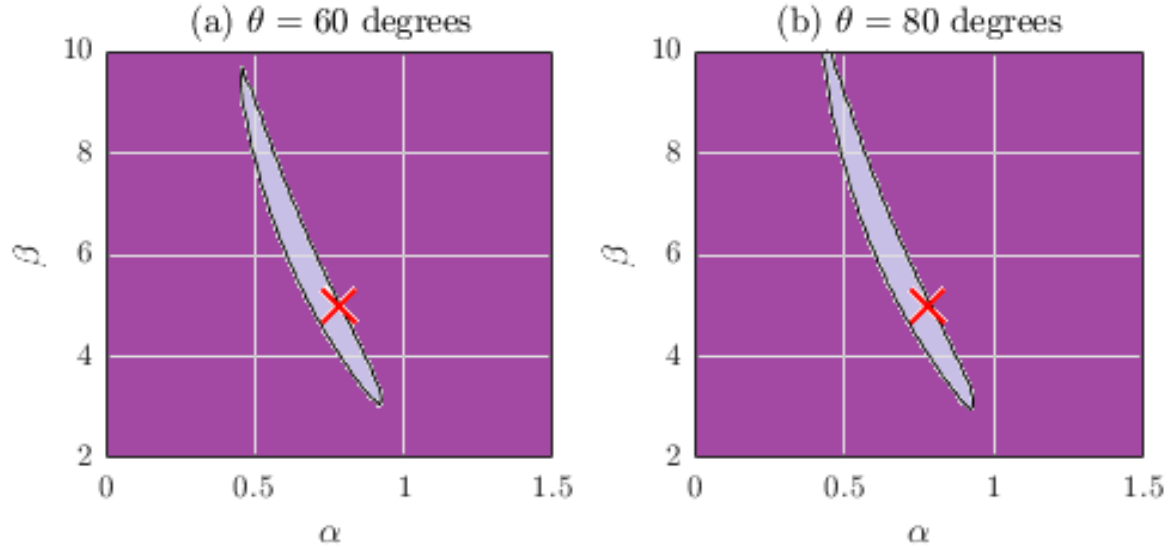

Figure 7.4: Neutral stability plots in the wavenumber state space for the pCf. The instability region is shown in light purple, with the dark purple region being the stable area. The red cross marks the most unstable point. The input parameters were $(Re, F_h) = (10000, 0.5)$ and (a) $\theta = 60$ degrees, (b) $\theta = 80$ degrees.

Now observing Figures 7.5 and 7.6 which were results for the pPf, there is a noticeably larger region of instability in the wavenumber state space with respect to the pCf. This is a particularly expected result as the unstratified pPf is more unstable than the pCf. Once again, by increasing the stratification (by reducing F_h), the region of instability grows, as found with the pCf. This can be seen as the unstable bubble is much larger for the respectively tilt angle between the two Figures.

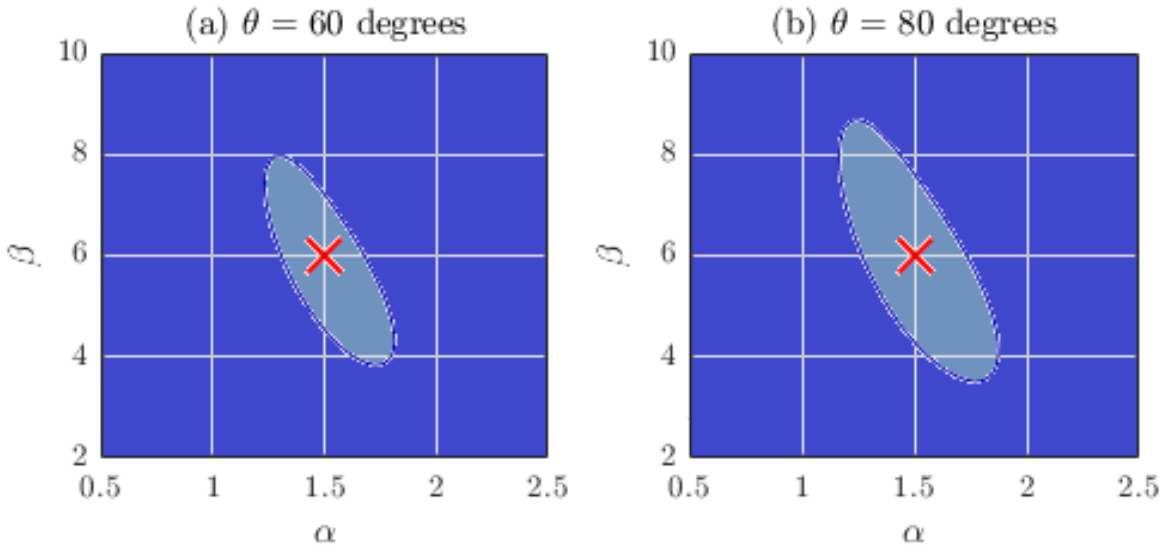

Figure 7.5: Neutral stability plots in the wavenumber state space for the pPf. The instability region is shown in light blue, with the dark blue region being the stable area. The red cross marks the most unstable point. The input parameters were $(Re, F_h) = (10000, 1)$ and (a) $\theta = 60$ degrees, (b) $\theta = 80$ degrees.

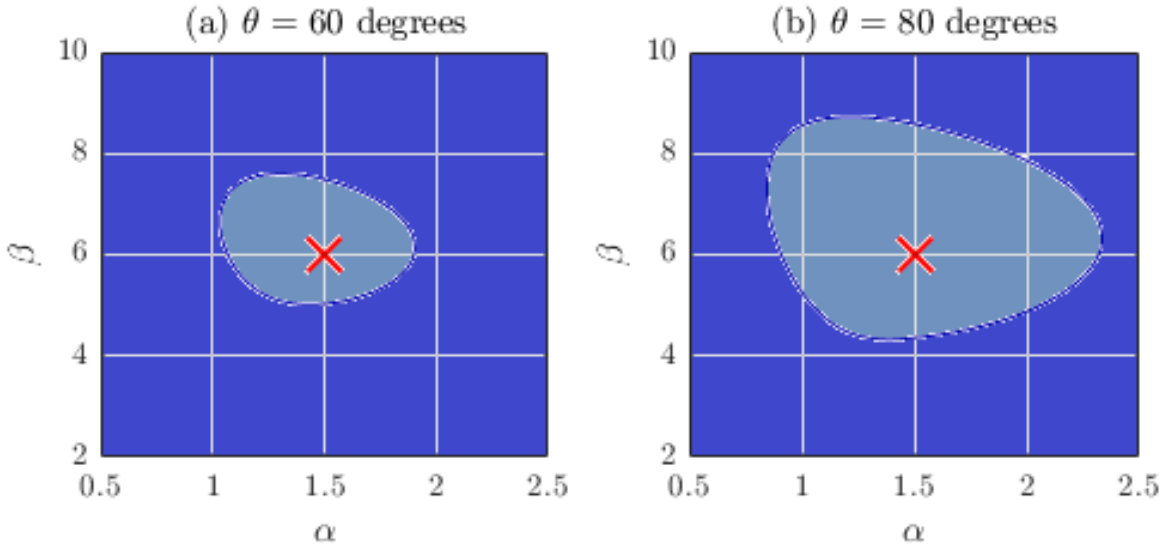

Figure 7.6: Neutral stability plots in the wavenumber state space for the pPf. The instability region is shown in light blue, with the dark blue region being the stable area. The red cross marks the most unstable point. The input parameters were $(Re, F_h) = (10000, 0.5)$ and (a) $\theta = 60$ degrees, (b) $\theta = 80$ degrees.

Likewise, as the tilt angle increases, the instability bubble grows. However, unlike the pCf, the most unstable region (marked with the red cross), is found around the centre of the instability region. This could suggests that at the critical tilt angle, the instability region is likely to be introduced at this point and then propagate in the wavenumber space as tilt angle is raised.

The most unstable region for the pCf was at the point $(\alpha, \beta) = (0.8, 5)$ (as found by Facchini) and $(1.5, 6)$ for the pPf.